

Received February 17, 2021; reviewed; accepted April 30, 2021

Proteomic profile to explain the mechanism of the *Bacillus cereus*-phosphate mineral interaction

Mai R. El-Ghammaz¹, Nagui A. Abdel-Khalek¹, Mohamed K. Hassan²

¹ Mineral Processing Department, Central Metallurgical Research and Development Institute (CMRDI), Cairo, Egypt

² Biotechnology Program, Zoology Department, Faculty of Science, Port-Said University, Egypt

Corresponding authors: mai.elghammaz@gmail.com (M. El-Ghammaz), mohamedkamel24@yahoo.com (M. Hassan)

Abstract: *Bacillus cereus* bacteria and their by-products were used as surface-active agents for surface hydrophobicity of the apatite in the flotation process leading to phosphate ores' enrichment. Recently, proteomics is used to investigate the biochemical processes through discovering new proteins or investigating protein-protein interactions. In this work, we investigated the physicochemical behavior of pure apatite and quartz minerals in the presence of *Bacillus cereus* using zeta-potential, FTIR, and hydrophobicity measurements. Our results indicated that isoelectric point (IEP) occurred at pH 4.7 for apatite and 2.1 for quartz mineral. *Bacillus cereus* treatment decreased IEP of apatite to 1.8; while there was no significant change in IEP value of quartz. We used comprehensive proteomic profile analysis of *Bacillus cereus* in the presence of apatite mineral to identify the biological mechanism and molecules involved in such enrichment capacity. Our data identified the up-regulated Surface Layer (S-Layer) protein in this bacterial strain to be associated with the best mineral yield.

Keywords: bio-flotation, phosphate, bacillus cereus, proteomic profile, S-layer protein

1. Introduction

Naturally occurring phosphate ores are the main source of phosphorous for fertilizers, animal food, and other chemicals (Hellal et al., 2019). The phosphorous is found as apatite or francolite mineral " $\text{Ca}_{10}(\text{PO}_4\text{CO}_3)_6\text{F}_2$ " (Samreen and Kausar, 2019). Phosphate mineral is mixed with other minerals (gangue). Yet, it requires better beneficiation processing to meet commercial specifications (Abdallah et al., 2018). Examples of well-known processing methods are flotation and selective flocculation. Flotation is a physicochemical separation process that utilizes the difference in surface properties of the valuable minerals and the unwanted gangue minerals. On the contrary, selective flocculation is to aggregate just the desired mineral particles (i.e., make them larger) and then separate (recover) the aggregates from the dispersed material. Hydrophobicity has to be imparted to minerals in order to float/flocculate them. In order to achieve this, different types of reagents, including oleic acid and amphoteric collector are used (Pattanaik and Venugopal, 2019; Ruan et al., 2019).

Recently, biological agents are becoming more alluring in mineral processing because of not only their low effective operating costs but also their possible applications to treat low-grade complex ores with difficult conditions/properties to beneficiate. Bio-beneficiation refers to the selective removal of undesirable mineral constituents from ore by utilizing bacteria as surface modifiers to enhance the separation with either flotation or flocculation (Dweyr et al., 2012; Teng et al., 2018). Biological processes of microbes or microbial fats and secreted metabolites can have specific interactions with minerals. Such interactions of microbes and their agents with minerals can be indirect, through biological products acting as surface-active agents, or direct due to microbial adhesion or attachment to the particles bringing out surface modification. Both types of interactions can lead to alteration of mineral hydrophobicity and, in some cases, cause flocculation or dispersion of mineral suspension. Bacteria can act as a surface modifier, depressant, collector, or dispersing agent to enhance the separation of minerals by either flotation or flocculation. Bacterial attachment to the mineral surface is an important step in

both flotation and flocculation. This attachment is affected mainly by the surface properties of both bacteria, and mineral, including surface charge, surface composition, and hydrophobicity (Tshikantwa et al., 2018; Cai et al., 2020; Chandra et al., 2020).

Bacteria-mineral interactions yield results that are relevant to various applications, including: i) adhesion of bacteria to mineral substrates resulting in biofilm formation; ii) bio-catalyzed oxidation, reduction, complexation, and precipitation reactions, and iii) reactions of bacterial cells and metabolic products with different mineral constituents in an ore matrix.

The end result of these biological processes is the formation and conversion of various mineral forms, surface modification and selective dissolution of mineral constituents, and bio-accumulation of dissolved metal ions. Mineral surface hydrophobicity can be brought about by controlled microbe-mineral interactions. Metabolic products as well as the bacterial cell components including cell wall and cell membrane can take part in these mineralogical reactions (Bruneel et al., 2019; Farghaly et al., 2021; Pereira et al., 2021).

Many studies have demonstrated the flocculation of minerals, sometimes selectively, by bacteria or substances derived from bacteria. *Mycobacterium phlei*, *Bacillus subtilis*, and soluble products obtained by sonication of the cells can function as flocculating agents where hematite can be selectively flocculated from silicates and coal from pyrite. In addition, *Corynebacterium sp.* are excellent flocculants for calcite and fluorite (Vijayalakshmi and Raichur, 2003; Smith and Miettinen, 2006). Extracellular bacterial proteins (EBP) derived from *Paenibacillus polymyxa* exhibited varying surface adsorption capacity towards minerals such as quartz, pyrite, chalcopyrite, galena, and sphalerite. Pyrite and chalcopyrite together could be effectively depressed while selectively floating galena, sphalerite, or quartz when mineral mixtures were preconditioned with the desirable identified protein fractions. Similarly, prior protein treatment resulted in the selective flocculation of pyrite-chalcopyrite, while galena, sphalerite, and quartz were effectively dispersed (Patra and Natarajan, 2008).

Several studies utilized the difference in surface properties between two minerals for selective attachment of bacteria. However, limited studies focused on the mechanism behind the surface properties alteration during the bacterial adsorption. The adhesion of *Bacillus subtilis* and *Mycobacterium phlei* onto dolomite and apatite was studied by sorption measurements and scanning electron microscopy and it was found that both *B. subtilis* and *M. phlei* adhered to dolomite more readily than onto apatite at acidic and near-neutral pH values (Abdallah et al., 2018; Derhy et al., 2020). Two strains of bacteria namely (*Corynebacterium- diphtheriae-intermedius*, *Pseudomonas Aeruginosa*) were used to modify dolomite and apatite surfaces and enhance the conventional flotation using an amphoteric collector. In 2018, *B. cereus* was isolated, for the first time, from phosphate mineral surface and its behavior was studied in mineral processing (Chandra et al., 2020).

In the last few years, proteomics has become one of the most powerful tools to investigate complex biochemical processes, discovery of new proteins, and investigation of protein-protein interactions involved in biotechnological applications. Proteomics involves the applications of technologies for the identification and quantification of the total protein content of a cell, tissue, or organism. It supplements the other "omics" technologies such as genomics and transcriptomics to expound the identity of proteins of an organism, and to cognize the structure and functions of a particular protein. Proteomics includes the analysis and categorization of overall protein signatures of a genome. Mass spectrometry with LC-MS/MS and MALDI-TOF/TOF being widely used equipment is the central among current proteomic analysis tool (Lee et al., 2020; Rodríguez et al., 2020).

In this study, we aimed to investigate the physicochemical behavior of a single pure apatite and quartz minerals. The proteomic profile analysis of *Bacillus cereus* in the presence of apatite mineral was studied and S-Layer protein was identified as a possible key player in minerals enrichment, thus increasing our understanding of the mechanism behind bacteria-mineral interaction.

2. Materials and methods

2.1. Materials

Chemicals and reagents: Pure single minerals (Apatite and Quartz) of purity 99.9% (Wards, USA) were employed in the fundamental study. All other chemicals including, NaOH, HCl, DDT (Dithiotheritol), and IAA (Iodoacetamide) used in this study were purchased from Sigma Aldrich, Germany. Analytical grades were used for the preparation of 0.1 M solutions (of NaOH or HCl) as pH regulators. Freshly

prepared nutrient broth/agar was used for the cultivation of bacterial strains. The agar was purchased from Lab M Limited (UK), while BCA kit (Bicinchoninic acid assay; Thermo Fischer Scientific, USA) working solutions, trypsin containing procaine enzyme were purchased from Sigma (Germany).

Bacterial strains: The bacterial sample wild type (WT) *Bacillus cereus* was supplied by the microbiology lab at Central Metallurgical R&D institute. *Bacillus cereus* was first isolated from the phosphate mineral surface and its behavior was studied in Mineral Processing Laboratory. *Bacillus cereus* was identified using both biochemical and molecular techniques (Biolog - 16S ribosomal RNA sequencing).

2.2. Methods

2.2.1. Bacterial propagation and maintenance

Using standard nutrient agar media, a loop full of the bacterial sample was inoculated on an agar plate by streak plate method followed by incubation at a temperature of 37°C for 24 hours then lyophilized and stored. A sterilized 350 ml nutrient broth was prepared in 1liter flask and used for bacterial incubation with a loop full of the bacterial isolate then incubated at 30°C for 24 hr. After overnight culturing, the optical density (OD) of the bacterial culture was measured, spectrophotometrically (LLG-UniSPEC Spectrophotometer). The OD is a method for calculating bacterial concentration. The turbidity for cell suspension is measured at a wavelength of 600 nm against culture medium as a reference, at which the 2.26 reading is equivalent to 14×10^7 CFU/ ml. This bacterial broth was used as a flotation reagent according to the method by Chandra et al. (2020).

2.2.2. Zeta potential measurements

A laser Zeta Meter 'Malvern Instruments Model Zeta Sizer 2000' was used for zeta potential measurements. A 0.05 g of the mineral was mixed with a definite concentration of the bacterial isolate in 50 ml of 2×10^{-2} M NaCl. The suspension was conditioned for 60 min during which the pH was adjusted (Farghaly et al., 2020).

2.2.3. FTIR measurements

FTIR spectra were recorded for apatite, silica, and bacteria before and after interactions using Fourier Transform Infrared Spectrometer (Model FT/IR 6300). The KBr pellet technique was used to record the spectra (Abdallah et al., 2018).

2.2.4. Bio-flotation experiments

A bench-scale flotation column of 100 ml volume was used for the floatability measurements. One gram of single mineral was conditioned at desired pH and specific bacterial concentration for 10 min using a horizontal shaker. Air-based flotation was conducted for 5 minutes using a flow-rate of 63 cm³/min. Both floated and sink fractions were collected, dried, weighted according to Farrokhpay et al., (2020).

2.2.5. Adaptation of *Bacillus cereus* to phosphate (adapted bacteria generation forming)

A 100 ml nutrient with a definite weight of phosphate mineral was mixed in a 250 ml flask and sterilized at 121°C for 20 min. A Bacterial broth was inoculated with a loop full of *Bacillus cereus* isolate as a control test then incubated at 30°C at 150 rpm shaking rate for 20 h, followed by a series of inoculations for the aforementioned bacterial broths. Each experiment was inoculated with 5ml of the previous bacterial isolate grown then incubated at 30°C at 150 rpm for 3-5 h (Deo and Natarajan, 1998). The bacterial population was determined as previously mentioned. This bacterial broth was used as a flotation reagent for the adapted group bio-flotation experiments.

2.2.6. Extraction, preparation, and quantification of proteins by non-targeting shotgun proteomics analysis

Wild type (WT) *Bacillus cereus* group and phosphate-adapted *Bacillus cereus* group were subjected to total protein extraction. One gram of apatite was conditioned at each desired pH and a specific bacterial concentration for 10 min. The suspended solution was centrifuged at 10000 rpm for 10-15 min at 4°C.

Then the supernatant was removed, while the bacterial pellets were kept at -80°C till used for further analysis. The protein content was extracted by vigorous shaking of the bacterial pellet with 8M urea solution, and then the pellet was centrifuged at 10000 rpm for 30 min at room temperature. Protein quantification was carried out, spectrophotometrically using Bicinchoninic acid assay (BCA assay) according to the manufacturer's recommendations. Briefly, the protein sample was incubated at 60°C for 30 min, then left to cool for 10 min, followed by spectrophotometer assessment at 562 nm (Bradford, 1976). Samples were then submitted to MS/MS-based proteomic profile analysis. The proteomic analysis and statistical analysis were performed at the proteomics and metabolomics unit at Children Cancer Hospital (CCHE-57357).

2.2.7. Protein precipitation

In case of low protein concentration yield, samples were subjected to precipitation and reconstitution in fewer amounts of 8M Urea. A certain volume of samples was transferred to a new tube, four times with chilled acetone. Samples were incubated at -80°C for 30 min, and then incubated at -20°C overnight. Centrifugation of the samples at 10000 rpm for 30 min was done. The supernatant was discarded and then left at room temperature (RT) till dryness. Pellets were reconstituted in 30 μl urea buffer.

2.2.8. Protein digestion, stage tip purification, and peptide quantification

Each Sample was digested using 0.2 M DDT (Dithiothreitol), vortexed, and then spun down. Samples were incubated for 45 min at room temperature (RT). A 2 μl of 1M IAA (Iodoacetamide) was added to each sample and incubated at RT for 45 min in the dark, followed by the addition of 102 μl of 0.1 M Tris pH 8.5 and then modified trypsin containing procaine enzyme was added and incubated overnight in a thermo-shaker at 900 rpm and 37°C for endopeptidase digestion (Magdeldin et al., 2014). The digested peptide solution was acidified using formic acid to pH 2-3 and spun down for 30 min at RT. The resultant peptide mixture was cleaned up using stage tip (Pierce™ C 18 Spin Tips) (Enany et al., 2017). A peptide quantification step was carried out using Bicinchoninic acid assay (BCA assay).

2.2.9. Nano-LC MS/MS analysis

Nano-LC MS/MS analysis was conducted using a TripleTOF 5600+ (AB Sciex, Canada). The most 40 abundant ions were sequentially selected in Information Dependent Acquisition (IDA) mode with a 2-5 charge state for high resolution for cycle time 1.5 sec (Magdeldin et al., 2014).

2.2.10. Proteomic data processing

Mascot generic format (mgf) files were created from raw data files using a script supplied by AB Sciex, Analyst TF 1.7.1 is used for data acquisition (Sciex software). MS/MS spectra were searched using X Tandem in Peptide shaker (version 1.16.45) against the Uniprot *Bacillus cereus* (swiss-prot) database containing (982,382 proteins) with reversed decoy sequences. To ensure high-quality results, the false discovery rate (FDR) was maintained at 1 % of the protein level.

2.2.11. Bioinformatic analysis of *Bacillus cereus*-phosphate mineral interaction

The biological processes and molecular functions of the identified proteins were obtained by searching through the Gene Ontology annotation (GO) database using the UniProtKB database (www.uniprot.org) and the Entrez PubMed database (www.ncbi.nih.gov).

2.2.12. Statistical analysis

To discriminate between the two groups involved in this study, we used volcano plot and T-test statistical tests. Data were considered statistically significant when P-value (Probability value) $P \leq 0.05$, unless otherwise stated. Where P-value is a number describing how likely it is that our data would have occurred under the null hypothesis of our statistical test (Saadeldin et al., 2020).

3. Results and discussion

3.1. Zeta potential of single minerals

As the first step of this study, we performed zeta potential for the minerals yielded from the interaction between *Bacillus cereus* and apatite and quartz single minerals. The zeta potential of apatite and quartz single minerals was determined over a wide range of pH, of which, the results were collected and shown in Fig. 1. Our results indicated that the point of intersection (isoelectric point) occurred at pH 4.7 for apatite and at pH 2.1 for quartz. The isoelectric point (IEP) of treated apatite with *Bacillus cereus* decreased from 4.7 to 1.8; while there is no significant change in the IEP value of quartz.

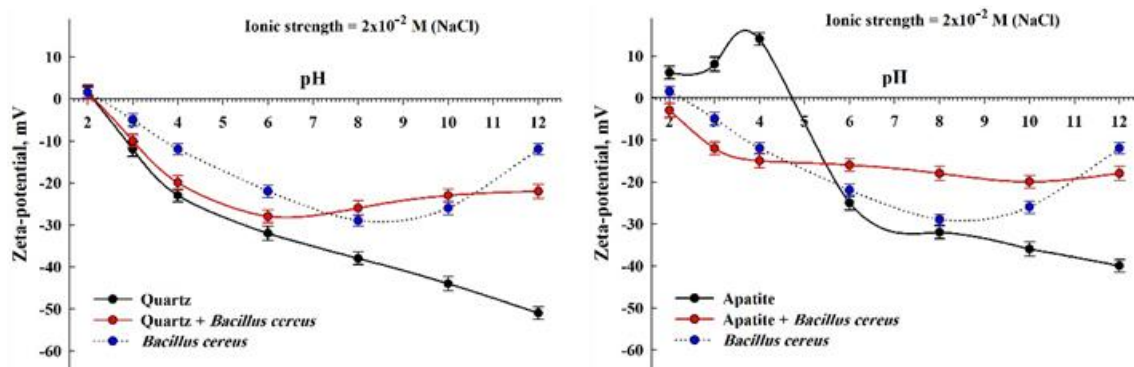


Fig. 1. Zeta-potential of single minerals (quartz and apatite) before and after treatment with *Bacillus cereus*

Bacterial attachment to any surface is related to surface charges on both the cells and the substratum. Charge separation can occur by dissociation of ionizable groups, such as $-\text{OH}$, $-\text{NH}$, $-\text{COOH}$, etc. The quartz as oxide mineral dissociated forming surface OH group thus, the surface becomes positively or negatively charged depending on the pH (Hamadi et al., 2008; Kinnunen et al., 2020). Negatively charged bacterial cells cannot overcome the energy barrier resulting from electrostatic repulsion; it may be deposited in the secondary minimum beyond the energy barrier. Long surface polymers of the cells may reach the solid surface across the energy barrier to achieve adhesion (Carniellom et al., 2018; Zaidi et al., 2018). A neutral macromolecule can also be adsorbed on charged or uncharged mineral surfaces. If the surface is charged, then adsorption of a biomolecule can cause a redistribution of the counter ion charge. This would lead to shifts in zeta potential. Therefore, on any hydrophilic surface, adsorption of exopolysaccharides (biofilm) can occur by strong hydrogen bonding between amino or carboxyl groups, peptide units, or ether as well as other polar groups on biological and mineral surfaces. The polysaccharides, consisting of several flexible sequences, may adopt different conformations at the mineral-solution interface (Limoli et al., 2015; Bruneel et al., 2019; Farghaly et al., 2021; Pereira et al., 2021). Similarly altering the surface hydrophobicity can bring about a difference in adsorption. Thus by changing one or more of the surface properties of the interacting surfaces, adsorption can be made more selective (Jiang et al., 2016; Attwood et al., 2019; Boudjema et al., 2020; Yu et al., 2020).

3.2. FTIR measurements

The bacteria are mainly composed of polysaccharides, lipids, and protein (Madigan et al., 2006; Vu et al., 2009; Lyu et al., 2020). The main characteristic peaks for *Bacillus cereus*, Fig. 2, are located at 1637.2 cm^{-1} which belongs to $\text{C}=\text{O}$ of the amide group and $\text{O}-\text{C}=\text{O}$ of carboxylate. This is besides the stretch vibration bands of $\text{O}-\text{H}$, $\text{N}-\text{H}$ at 2075.0 and 3440.3 cm^{-1} .

On the interaction between *Bacillus cereus* and apatite mineral, new functional groups are observed (Fig. 2). The treated apatite mineral formed a hydrogen bond with *Bacillus cereus*, which is confirmed by $\text{C}-\text{H}$ and at 642 cm^{-1} and with $\text{C}=\text{C}-\text{H}$, $\text{C}-\text{H}$ at 2932 cm^{-1} . Also, the treatment caused a band shift from 3340.3 to 3443.7 cm^{-1} due to the interaction of (OH^-) of polysaccharides of the metabolites and the positive adsorption sites of the apatite surface (Kinnunen et al., 2020; Yap et al., 2020; Farghaly et al., 2021). The disappearance of $\text{C}=\text{O}$ amide function group at 1637.2 cm^{-1} confirms the interaction of the amide group and the positively charged sites of apatite (Yang et al., 2020).

Furthermore, in case of quartz, our data revealed new species of functional groups which were detected as a result of the treatment with *Bacillus cereus* at 2326 cm^{-1} for the carboxylic acid, 1080 cm^{-1}

for C–O stretch of ether group and at 784 cm^{-1} for C–H and C=C of the phenyl group. The electrostatic interaction between the negative silanol groups on the quartz surface with the positive amino (NH_2) groups of bacteria is confirmed by the disappearance of the sharp peak of amino groups at 1637.2 cm^{-1} (Fig. 3). Therefore, the type of adsorption that occurred is mainly chemical adsorption, which makes the apatite's surface more hydrophobic than the quartz's surface and, ultimately, enhances its separation.

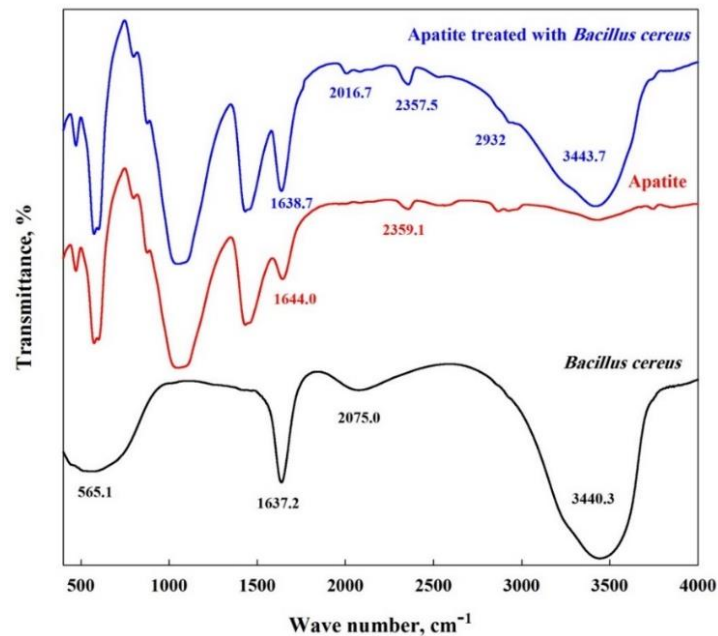


Fig. 2. FTIR spectra of apatite mineral, *Bacillus cereus*, and apatite mineral after treatment with *Bacillus cereus*

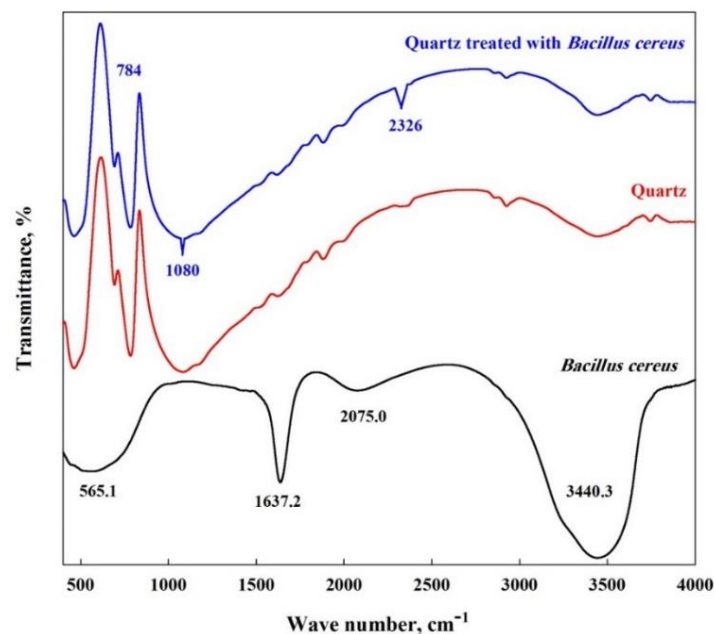


Fig. 3. FTIR spectra of quartz mineral, *Bacillus cereus*, and quartz mineral after treatment with *Bacillus cereus*

These results run in agreement with the zeta potential and the adhesion measurement and with the preceding work (Combes et al., 2006; Michelot et al., 2015; Sarvamangala et al., 2017; Selim and Rostom, 2018; Mokhtar et al., 2020). The adsorption of protein (amino acids) products of *Bacillus cereus* onto the apatite is responsible for the higher adsorption affinity to the apatite surface, in comparison to quartz. On the other hand, the weak adsorption of polysaccharides to apatite surface, in comparison to quartz is the reason for no significant effect on minerals behavior (Abdallah et al., 2018).

3.3. Bio-flotation of single minerals

As for the bio-flotation experiments, these experiments were performed at different operating conditions such as bacterial concentration, conditioning time, and pH. Fig. 4 reflects that the floatability of apatite, at optimum bacterial concentration and conditioning time, increased with increasing the pH to reach its maximum value (96%) at pH 5-8; then decreased again. On the contrary, the floatability of quartz decreased with increasing the pH to reach its minimum value (14-18%) at pH 6-7.

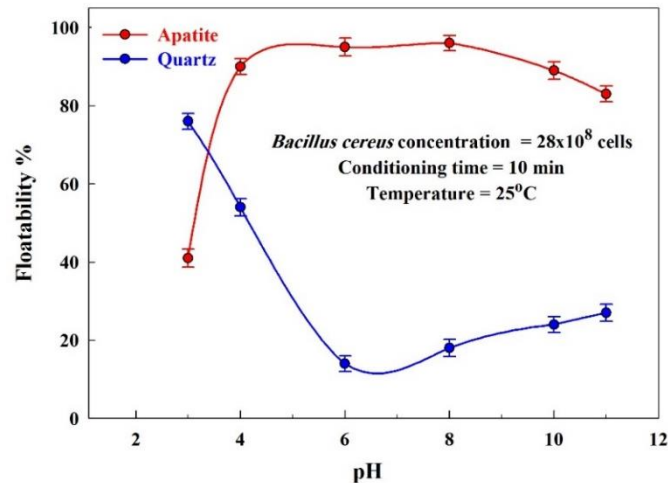


Fig. 4. Effect of pH on the floatability of quartz and apatite

The maximum floatability of apatite compared to quartz is due to the higher affinity of *Bacillus cereus* to apatite than quartz. The adsorption of bacteria onto apatite at pH 6 is attributed to electrostatic forces, hydrogen bonding, and chemical interaction (Jiang et al., 2004; Nimmagadda et al., 2017; Abdallah et al., 2018). The floatability of apatite and quartz increased with increasing the bacterial concentration. The apatite showed higher floatability than quartz. Also, at higher bacterial concentrations, the floatability of apatite decreased again. This is due to the adsorption of protein (amino acids) of *Bacillus cereus* onto the apatite which is responsible for the higher adsorption affinity to apatite surface, in comparison to quartz. On the other hand, the weak adsorption of polysaccharides to apatite surface, in comparison to quartz is the reason for no significant effect on minerals behavior (Abdallah et al., 2018).

The higher floatability at long conditioning time is because the particle and bubble attachment is not instantaneous, which is referred to as induction time. Induction time is associated with the properties of the thin water film that separates the particle and the bubble just before the attachment. For a hydrophobic surface, induction time is short, a few milliseconds, and if it is less than the time the particle and bubble are in contact, attachment is successful and the particle is floated. With a hydrophilic surface, the induction time is large and exceeds the particle bubble contact time. The induction time is used to characterize surface properties related to flotation. The adsorption of bacteria on the mineral surface includes the presence of surface appendages, cell surface, and exopolymers. Appendages are mostly protein and may bind to specific molecules available on the mineral surfaces (Dweyr et al., 2012; Ramírez-Aldaba et al., 2017; Li et al., 2018; Teng et al., 2018).

3.4. Proteomic profile analysis

In our study, to investigate the interaction of *Bacillus cereus* with phosphate mineral on the level of protein expression and to identify the potential molecules involved in the best mineral enrichment, the proteomic profile of *Bacillus cereus* during interaction with the phosphate mineral was compared by MS/MS analysis at different experimental point (different pH). For that purpose, bio-flotation experiments were performed using the bacterial samples (Wild Type (WT) *Bacillus cereus* & the phosphate mineral adapted *Bacillus cereus*) as a flotation agent for the phosphate ore at optimum bacterial concentration and conditioning time. Following the conditioning steps, the protein samples were extracted according to the protocol as mentioned before in Section (2.2.6). The proteomic profile samples, that were collected, were related to the bio-flotation experiments done using the following conditions: i) Wild Type (WT) *Bacillus cereus* bacteria (as a control); ii) Wild Type (WT) *Bacillus cereus*

bacteria conditioned together with phosphate mineral (bio-flotation experiments at different pH); iii) phosphate mineral adapted *Bacillus cereus* bacteria(as a control), and iv) The phosphate mineral adapted *Bacillus cereus* bacteria conditioned together with phosphate mineral(bio-flotation experiments at different pH). The proteomic profile of these samples, together with the investigation of the identified proteins, provided high-confidence datasets of identified proteins. The *Bacillus cereus* WT samples and the *Bacillus cereus* adapted samples resulted in the identification of numerous proteins listed in Table1.

Table 1. List of the identified proteins' count in test samples

Sample description	Identified Proteins (No.)
<i>Bacillus cereus</i> WT (BC WT)	1340
BC WT with Apatite at natural pH	41
BC WT with Apatite at pH=5	334
BC WT with Apatite at pH=7	571
BC WT with Apatite at pH=10	57
BC WT adapted to Apatite (Adpt.)	1335
BC WT (Adpt.) at natural pH	603
BC WT (Adpt.) at pH=5	348
BC WT (Adpt.) at pH=7	677
BC WT (Adpt.) at pH=10	320

Then the lists of proteins were filtered and the proteins that have less than 50% abundance were excluded followed by normalization using probabilistic quotient normalization (PQN) then log-transformation, and auto-scaling. The top 58 proteins were distributed into up-regulated, down-regulated, and no-change proteins according to Log 2 fold change as illustrated in Fig. 5. The up-regulated and the down-regulated were chosen according to the significance of the fold change value. From the shared proteins between *Bacillus cereus* WT and *Bacillus cereus* Adapted, significantly different proteins were selected by volcano plot with the $-\text{Log}_{10}$ (P-value) and the magnitude of difference (Log2) in expression value between average biological replicates of the two groups (Fig .6). Data were subjected to an unpaired T-test and the significant output was considered only when $p \leq 0.05$ (Fig .7).

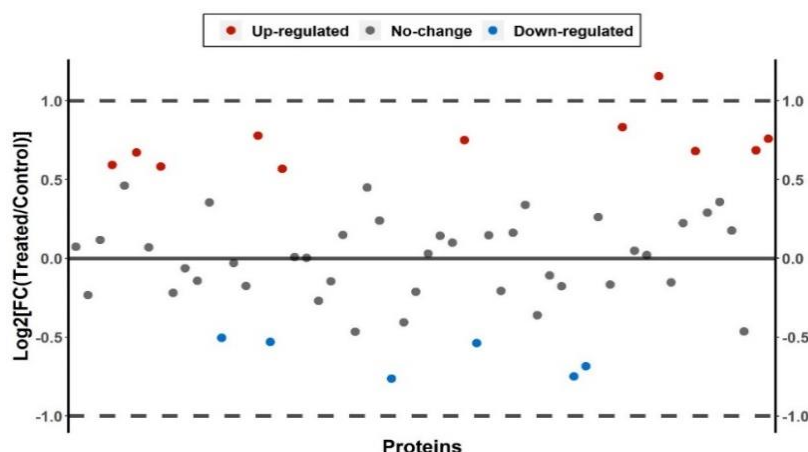


Fig. 5. The distribution of the identified proteins into up-regulated, down-regulated, and no-change proteins according to Log 2 fold change

3.4.1. Potentially involved proteins in mineral enrichment

The specific expression changes of the proteins with evident variations were depicted in the heat map (Fig. 8). When compared with each other, the protein content showed appreciated variation among them, which indicates the bacterial response towards the presence of phosphate mineral. Also, the heat

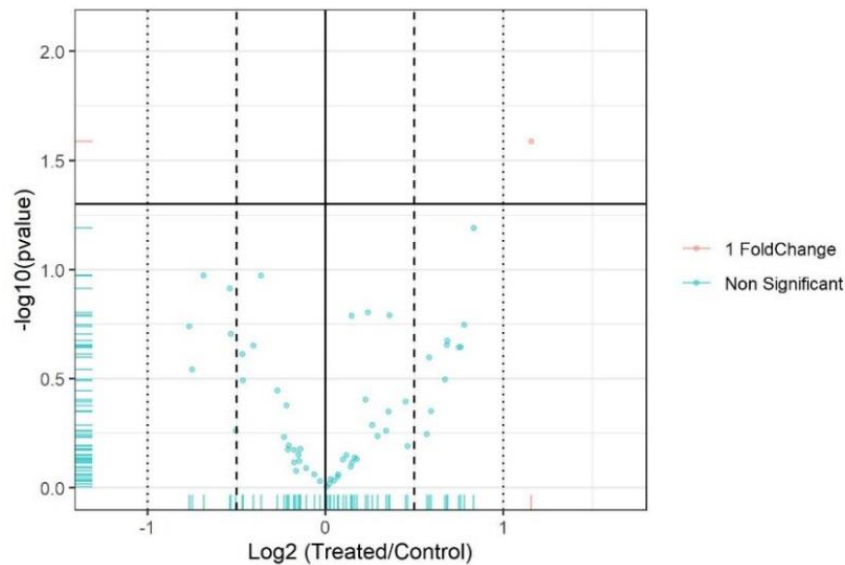


Fig. 6. Volcano plot showing the statistical significance of the identified proteins resulting from the two groups (wild type *Bacillus cereus* group and *Bacillus cereus* adapted to phosphate mineral group)

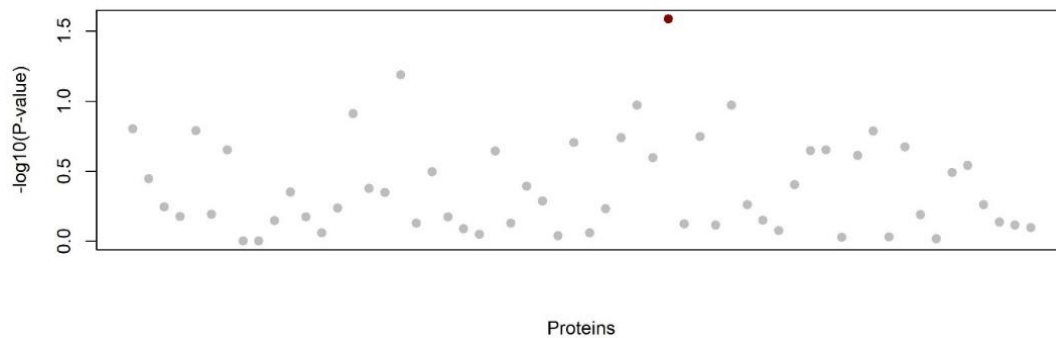


Fig. 7. T-test indicating the most significant protein (A0A329FFT6) among all of the identified proteins according to $-\text{Log}_{10}(\text{P-value})$

map shows protein expression variations between WT *Bacillus cereus* samples and *Bacillus cereus*-adapted samples.

From all the bacterial proteins, 58 proteins were differentially expressed between different experimental groups. Among these proteins, 17 proteins showed a significant difference in their expression ($p \leq 0.05$). The differential expression revealed 11 proteins as up-regulated and 6 proteins as downregulated in WT *Bacillus cereus* when compared with adapted *Bacillus cereus*. These results helped us propose such upregulated proteins as candidate molecules associated with phosphate (Table 2). The heat-map between these two groups summarizes this list of proteins and reflects the fold change of proteins (Fig. 8).

Categorization of these proteins, through Gene Ontology annotation, identified unique protein/s, assigned to a specific function and biological process together with the molecular functions. Function annotations included translation, carbohydrate metabolic activity, DNA replication, ion transport, stress proteins, and protein folding. Moreover, some of the identified up-regulated proteins were found to be involved in protein synthesis, cell division, and stress proteins. While some of the down-regulated proteins are related to metalloproteases, protein folding, and metal ion binding. Interestingly, one of the most significantly up-regulated proteins in the adapted bacterial colony is the Surface layer (S-Layer) protein with 1.156 fold change (Table 2).

The up-regulated S-layer protein suggested the involvement in the response of *Bacillus cereus* to the phosphate mineral. Importantly, this S-layer protein showed no significant change with the different pH conditions suggesting that such increase is mainly due to the phosphate mineral amount/adaptation but not pH as shown in the heat map within the same group.

Table 2. The identified proteins according to their Status

Accession No.	Status	Fold Change	Protein Name	Gene Name
A0A068N328	Up-regulated	0.568344	Tellurium resistance protein	BcrFT9_00428
A0A063CE22		0.592699	50S ribosomal protein L23	rplW
A0A158RTL5		0.833185	Camelysin	calY
A0A063CIP2		0.671677	50S ribosomal protein L7/L12	rplL
A0A0E1MIT6		0.75042	Cell division protein FtsN	B2J90_06905
A0A063CJG9		0.582048	Dihydrolipoyl dehydrogenase	lpdA
A0A329FFT6 *		1.156088	S-layer protein	A6E21_08465
A0A063CUX6		0.778068	Nucleoside diphosphate kinase	ndk
Q816H3		0.759282	Cold shock-like protein CspD	cspD
J7ZXA3		0.681139	S-layer protein sap	IG7_00714
Q636T3		0.685695	Group-specific protein	BCE33L3502
A0A0G8DDD7		Down-regulated	-0.53713	Probable manganese-dependent inorganic pyrophosphatase
A0A068N2U8	-0.53037		DNA-directed RNA polymerase subunit beta	rpoB
A0A0B5ZI75	-0.76379		Chaperone protein DnaK	dnaK
A0A150B0G0	-0.68377		Penicillin-binding protein	AT274_13750
A0A063CMS9	-0.50415		50S ribosomal protein L31 type B	rpmE2
A0A150AWC1	-0.74950		Neutral metalloproteinase	AT274_10670

(*) Indicating the most significant protein with $-\log_{10}$ (P-value) equals 1.5866429. This value was obtained using statistical calculations that were summarized and illustrated in Figs. 5, 6, 7

3.4.2. S-Layer protein structure

The S-Layer protein is 86.348 kDa in molecular weight and belongs to the Surface layer homology (SLH) family. S-Layer protein consists of 813 amino acids, and the sequence was identified using the uniprot. database. The protein sequence alignment for the S-layer protein matched with the S-Layer protein Surface array protein (Sap) of *Bacillus anthracis* with 95.9%. The SLH domains of *Bacillus cereus*: SLH₁, SLH₂, and SLH₃ were found at the N-terminus of the protein at the positions 33-75, 93-135, and 155-196, respectively, suggesting that the N-terminus is involved in the anchoring of the S-layer to the cell wall components (Suhr et al., 2016). Recent structural studies have revealed that several S-layer subunits share a region of homology in a domain that has been shown to interact with the cell wall (Dramsai and Bierne, 2017; Chandramohan et al., 2020). All SLH domains identified thus far have been found at the very beginning or end of the mature proteins. An SLH domain is usually composed of either a single or three repeating SLH motifs of approximately 50 to 60 residues (Dramsai and Bierne, 2017; Chandramohan et al., 2020). Secreted proteins encoding three tandem SLH domains are tethered to the bacterial envelope by non-covalent interactions between the SLH domains and a secondary cell wall carbohydrate (Bharat et al., 2020). S-layers are stabilized by divalent cations, such as Ca²⁺ ions, and thus contribute to the cohesion of the proteins by electrostatic interactions (Chandramohan et al., 2020).

The S-layer proteins are non-covalently linked to silicon or other supporting structures with differing combinations of weak bonds (hydrophobic bonds, ionic bonds involving divalent cations or direct interaction of polar groups, and hydrogen bonds), and are responsible for the structural integrity as well. Nevertheless, disintegration and reassembly experiments led to the conclusion that the bonds holding the S-layer proteins together must be much stronger than those binding them to the support. The proteomic analysis of *Bacillus cereus* during interaction with the phosphate mineral showed that the outer surface of bacteria is coated with a protein surface layer which has important roles in many functions (Germino et al., 2015; Chandramohan et al., 2020).

3.4.3. S-Layer protein function

The up-regulation of the S-Layer protein for phosphate mineral indicates the involvement of the S-Layer protein in the bacteria-mineral interaction during the bio-flotation process. This study may trigger the

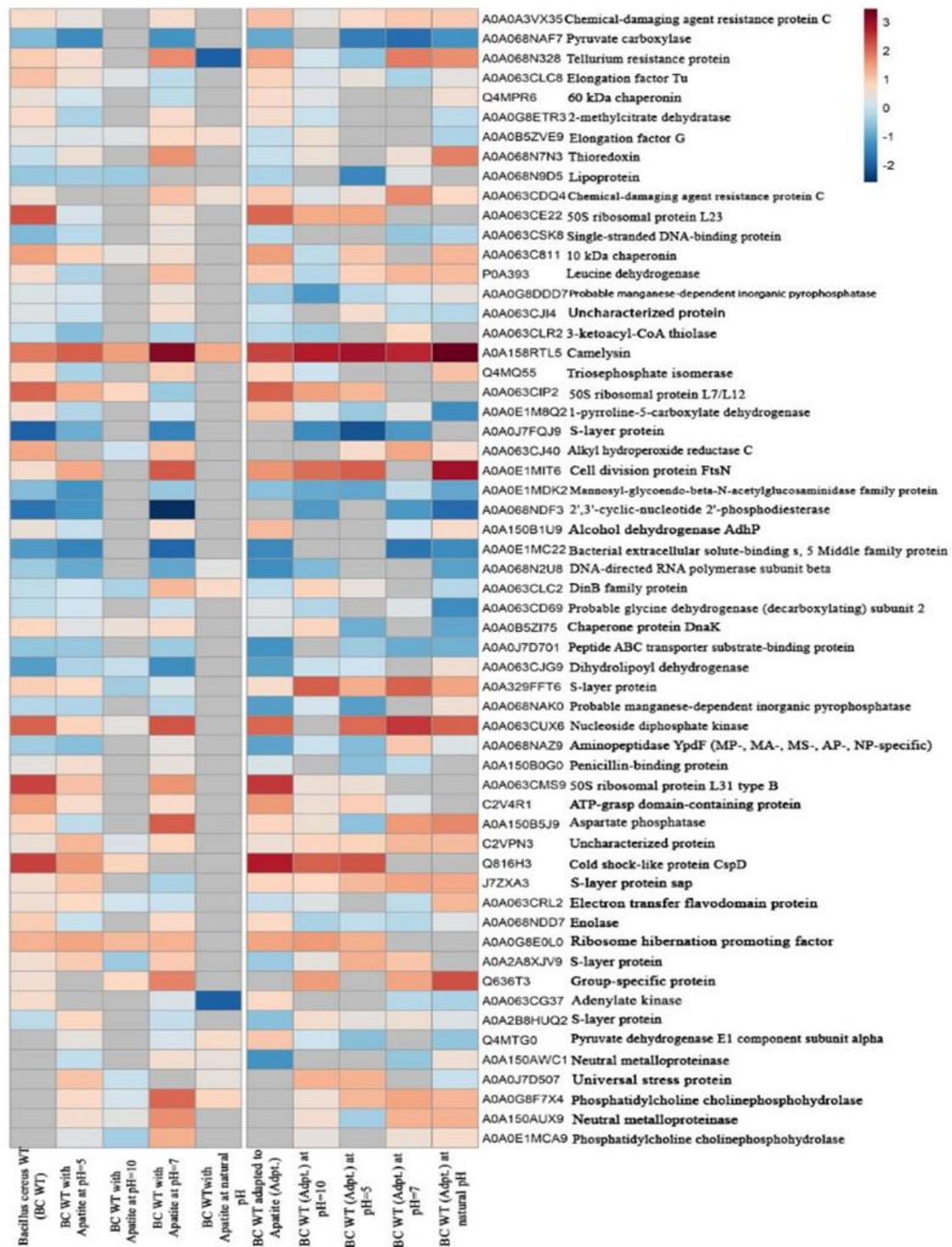


Fig. 8. Heat-map shows the differential protein expression in different groups. The left heat-map represents the protein expression of wild-type *Bacillus cereus* with phosphate mineral at different pH, and the right represents protein expression of *Bacillus cereus* adapted to phosphate mineral at different pH

future potentiality of biotechnological application for the industry. The S-layer protein is also known to be involved in cell surface hydrophobicity and adhesion of *Bacillus cereus* to biotic and abiotic surfaces (Kimkes and Heinemann, 2020).

This interaction may be due to a defense mechanism against harsh conditions or a tendency to favorable ones. The adhesion of bacteria to the phosphate mineral might be an innate anchoring behavior towards support surfaces, or a tendency of the microorganisms towards needed minerals and elements. The real reason for this reaction is yet to be discovered. Once formed, S-layer proteins were

never leaving the lattice, and thus, it was concluded that lattice growth is irreversible and no S-layer protein turnover occurs (Chandramohan et al., 2020).

The intrinsic properties and physiological functions of the S-layer proteins build the base for its selective metal binding behavior and its potential for the fabrication of bio-hybrid materials. So by the combination of S-layers with well-known sorption materials, functional coatings or composite materials with improved properties can be developed (Vogel et al., 2017).

The aforementioned significant protein is one of the S-layers proteins that are para-crystalline bi-dimensional arrays of proteins or glycoproteins that overlay the cell surface of several genus and species of bacteria and archaea. As the outermost layer of several genus and species of microorganisms, S-layer proteins are in direct contact with the bacterial environment and thus may be involved in many of their surface properties, including adherence to various substrates, mucins, and eukaryotic cells, aggregation, and co-aggregation with yeasts and other bacteria. In addition, S-layer proteins have been reported to be responsible for bacterial protection against detrimental environmental conditions and to play an important role in surface recognition or as carriers of virulence factors. Also, the intrinsic properties and physiological functions of the S-layer proteins were found to cause selective metal binding and release behavior by the S-layer protein monomer (Vogel et al., 2017).

These results propose a role for the S-layer protein, for the first time, as a key player in mineral enrichment by bacteria which opens a different understanding of the interaction between the bacterial S-Layer protein and the natural phosphate mineral.

4. Conclusions

Our results indicated that the point of intersection (isoelectric point) occurred at pH 4.7 for apatite and at pH 2.1 for quartz. The isoelectric point (IEP) of treated apatite with *Bacillus cereus* decreased from 4.7 to 1.8; while there is no significant change in IEP value of quartz. The higher floatability of apatite compared to quartz might be due to the higher affinity of *Bacillus cereus* to apatite than quartz. The adsorption of bacteria onto apatite is attributed to electrostatic forces, hydrogen bonding, and chemical interaction. The surface proteins of *Bacillus cereus* mediate the higher adsorption affinity to the apatite surface. Moreover, the comparative proteomic profiling of *Bacillus cereus* in the presence of apatite mineral identified, for the first time at least in this species, the up-regulated S-Layer, Sap, proteins as a potential candidate molecule. This S-Layer protein may play a role in mineral enrichment because of its surface properties, including the adherence to various substrates, and the direct contact with the bacterial environment. These data pave the way for a deeper understanding of the possible role of the S-Layer protein in the interaction of the bacteria with the natural phosphate mineral. Further genetic-based manipulations including cloning and overexpression or deletion could be used to study how these manipulations will affect the phosphate yield by enhancing the efficiency of bacteria, which may lead to the industrialization of bacterial cells as a biological agent for the bio-flotation process.

Acknowledgments

The authors acknowledge Central Metallurgical Research & Development Institute (CMRDI), Helwan, Cairo, Egypt, for providing the necessary facilities to carry out the research work. The authors also declare that this research received no external funding.

References

- ABDALLAH, S.S., EL-SHATOURY, E.H., ABDEL-KHALEK, N.A., YOUSSEF, M.A., SELIM, K.A., IBRAHIM, M.K., ELSAYED, S.M., 2018. *Bio-Flotation of Egyptian Siliceous Phosphate Ore Using Bacillus cereus*. Proceedings of the 4th World Cong. Mech., Chem. & Mater. Eng. (MCM'18), Spain, 2018, MMME 114, 1-8.
- ATTWOOD, S.J., KERSHAW, R., UDDIN, S., BISHOP, S.M., WELLAND, M.E., 2019. *Understanding how charge and hydrophobicity influence globular protein adsorption to alkanethiol and material surfaces*. Journal of Materials Chemistry B, 7(14), 2349-2361.
- BHARAT, T.A., VON KÜGELGEN, A., ALVA, V., 2020. *Molecular Logic of Prokaryotic Surface Layer Structures*. Trends in microbiology, 10,1-11.

- BOUDJEMA, L., LONG, J., PETITJEAN, H., LARIONOVA, J., GUARI, Y., TRENS, P., SALLES, F., 2020. *Adsorption of volatile organic compounds by ZIF-8, Cu-BTC and a Prussian blue analogue: A comparative study*. Inorganica Chimica Acta, 501, 119316, ISSN 0020-1693.
- BRADFORD, M.M., 1976. *A rapid and sensitive method for the quantitation of microgram quantities of protein utilizing the principle of protein-dye binding*. Analytical biochemistry, 72(1-2), 248-54.
- BRUNEEL, O., MGHAZLI, N., SBABOU, L., HÉRY, M., CASIOT, C., FILALI-MALTOUF, A., 2019. *Role of microorganisms in rehabilitation of mining sites, focus on Sub Saharan African countries*. Journal of Geochemical Exploration, 205, 106327.
- CAI, S., WU, C., YANG, W., LIANG, W., YU, H., LIU, L., 2020. *Recent advance in surface modification for regulating cell adhesion and behaviors*. Nanotechnology Reviews, 9(1), 971-989.
- CARNIELLOM, V., PETERSON, B.W., VAN DER MEI, H.C., BUSSCHER, H.J., 2018. *Physico-chemistry from initial bacterial adhesion to surface-programmed biofilm growth*. Advances in Colloid and Interface Science, 261, 1-14.
- CHANDRA, P., ENESPA, SINGH, R., ARORA, P.K., 2020. *Microbial lipases and their industrial applications: a comprehensive review*. Microb Cell Fact, 19(169), 1-42.
- CHANDRAMOHAN, A., DUPRAT, E., REMUSAT, L., ZIRAH, S., LOMBARD, C., KISH, A., 2020. *Novel mechanism for surface layer shedding and regenerating in bacteria exposed to metal-contaminated conditions*. Frontiers in microbiology, 9, 3210.
- COMBES, C., CAZALBOU, S., REY, C., 2016. *Apatite Biominerals*. Minerals, 6(2), 34.
- DEO, N., NATARAJAN, K.A., 1998. *Studies on interaction of Paenibacillus polymyxa with iron ore minerals in relation to beneficiation*. International Journal of Mineral Processing, 55(1), 41-60.
- DERHY, M., TAHA, Y., HAKKOU, R., BENZAAZOUA, M., 2020. *Review of the Main Factors Affecting the Flotation of Phosphate Ores*. Minerals, 10, 1109.
- DRAMSI, S., BIERNE, H., 2017. *Spatial Organization of Cell Wall-Anchored Proteins at the Surface of Gram-Positive Bacteria*. Curr Top Microbiol Immunol, 404, 177-201.
- DWEYR, R., BRUCKARD, W.J., REA, S.M., HOLMES, R.J., 2012. *Bioflotaion and bioflocculation review, Microorganisms relevant from mineral beneficiation*. Mineral processing and Extractive Metallurgy IMM Transactions section C, 21(2), 65-71.
- ENANY, S., YOSHIDA, Y., TATEISHI, Y., OZEKI, Y., NISHIYAMA, A., SAVITSKAYA, A., YAMAGUCHI, T., OHARA, Y., YAMAMOTO, T., ATO, M., MATSUMOTO, S., 2017. *Mycobacterial DNA-binding protein 1 is critical for long term survival of Mycobacterium smegmatis and simultaneously coordinates cellular functions*. Scientific reports, 7(1), 1-11.
- FARGHALY, M.G., ABDEL-KHALEK, N.A., ABDEL-KHALE, M.A., SELIM, K.A., ABDULLAH, S.S., 2021. *Physicochemical study and application for pyrolusite separation from high manganese-iron ore in the presence of microorganisms*. Physicochemical Problems of Mineral Processing, 57(1), 273-283.
- FARROKHPAY, S., FILIPPOV, L., FORNASIERO, D., 2020. *Flotation of Fine Particles: A Review*. Mineral Processing and Extractive Metallurgy Review, 155, 1-11.
- GERBINO, E., CARASI, P., MOBILI, P., SERRADELL, M.A., GÓMEZ-ZAVAGLIA, A., 2015. *Role of S-layer proteins in bacteria*. World Journal of Microbiology and Biotechnology, 12, 1877-1887.
- HAMADI, F., LATRACHE, H., ZAHIR, H., ELGHMARI, A., TIMINOUNI, M., ELLOUALI, M., 2008. *The relation between Escherichia coli surface functional groups' composition and their physicochemical properties*. Brazilian Journal of Microbiology, 39(1), 10-15.
- HELLAL, F., EL-SAYED, S., ZEWAINY, R., AMER, A., 2019. *Importance of phosphate rock application for sustaining agricultural production in Egypt*. Bulletin of the National Research Centre, 43(1), 1-11.
- JIANG, W., SAXENA, A., SONG, B., WARD, B.B., BEVERIDGE, T.J., MYNENI, S.C.B., 2004. *Elucidation of Functional groups on gram positive and gram negative bacterial surfaces using infrared spectroscopy*. Langmuir, 20(26), 11433-11442.
- JIANG, H.R., CHAN, D.C., 2016. *Superhydrophobicity on nanostructured porous hydrophilic material*. Appl. Phys. Lett., 108(17), 171603.
- KIMKES, T.E., HEINEMANN, M., 2020. *How bacteria recognise and respond to surface contact*. FEMS microbiology reviews, 44(1), 106-122.
- KINNUNEN, P., MIETTINEN, H., BOMBERG, M., 2020. *Review of Potential Microbial Effects on Flotation*. Minerals, 10(6), 533.
- LEE, P.Y., SARAYGORD-AFSHARI, N., LOW, T.Y., 2020. *The evolution of two-dimensional gel electrophoresis-from proteomics to emerging alternative applications*. Journal of Chromatography A, 1615, 460763.

- LI, Q., DONG, F., DAI, Q., ZHANG, C., YU, L., 2018. *Surface properties of PM2.5 calcite fine particulate matter in the presence of same size bacterial cells and exocellular polymeric substances of Bacillus mucitagnosus*. Environ. Sci. Pollut. Res. Int., 25(23), 22429-22436.
- LIMOLI, D.H., JONES, C.J., WOZNIAK, D.J., 2015. *Bacterial Extracellular Polysaccharides in Biofilm Formation and Function*. Microbial Biofilms, 3(3), 223-247.
- LYU, Z., SHANG, Y., WANG, X., WU, Y., ZHENG, J., LIU, H., GONG, T., YE, L., DI, Q., 2020. *Monoclonal Antibodies Specific to the Extracellular Domain of Histidine Kinase YycG of Staphylococcus epidermidis Inhibit Biofilm Formation*. Frontiers in Microbiology, 11, 1839.
- MADIGAN, M.T., MARTINKO, J.M., BROCK, T.D., 2006. *Brock biology of microorganisms*. Upper Saddle River, NJ: Pearson Prentice Hall. 11th Ed. ISBN:0130491470.
- MAGDELDIN, S., ENANY, S., YOSHIDA, Y., XU, B., ZHANG, Y., ZUREENA, Z., LOKAMANI, I., YAOITA, E., YAMAMOTO, T., 2014. *Basics and recent advances of two dimensional-polyacrylamide gel electrophoresis*. Clinical proteomics, 11(1), 16.
- MAGDELDIN, S., YAMAMOTO, T., TOOYAMA, I., ABDELALIM, E.M., 2014. *New proteomic insights on the role of NPR-A in regulating self-renewal of embryonic stem cells*. Stem Cell Reviews and Reports, 10(4), 561-72.
- MICHELOT, A., SARDA, S., AUDIN, C., DEYDIER, E., MANOURY, E., POLL, R., REY, C., 2015. *Spectroscopic characterization of hydroxylapatite and nanocrystalline apatite with grafted amino-propyl-triethoxysilane: nature of silane-surface interaction*. Journal of Materials Science, 50(17), 5746- 5757.
- MOKHTAR, A., ABDELKRIM, S., HACHEMAOUI, M., ADJDIR, M., ZAHRAOUI, M., BOUKOUSSA, B., 2020. *Layered silicate magadiite and its composites for pollutants removal and antimicrobial properties: A review*. Applied Clay Science, 198, 105823.
- NIMMAGADDA, A., LIU, X., TENG, P., SU, M., LI, Y., QIAO, Q., KHADKA, N.K., SUN, X., PAN, J., XU, H., LI, Q., CAL, J., 2017. *Polycarbonates with Potent and Selective Antimicrobial Activity toward G-Positive Bacteria*. Biomacromolecules, 18 (1), 87-95.
- PATRA, P., NATARAJAN, K.A., 2008. *Role of mineral specific bacterial proteins in selective flocculation and flotation*. International Journal of Mineral Processing, 88(1-2), 53-58.
- PATTANAİK, A., VENUGOPAL, R., 2019. *Role of Surfactants in Mineral Processing: An Overview*. In Surfactants and Detergents, DUTTA, A.K., IntechOpen, 1-17.
- PEREIRA, A.R.M., HACHA, R.R., TOREM, M.L., MERMA, A.G., SILVAS, F.P., ABHILASH, A., 2021. *Direct hematite flotation from an iron ore tailing using an innovative biosurfactant*. Separation Science and Technology, In press, 1-11.
- RAMÍREZ-ALDABA, H., VAZQUEZ-ARENAS, J., SOSA-RODRÍGUEZ, F.S., VALDEZ-PÉREZ, D., RUIZ-BACA, E., GARCÍA-MEZA, J.V., TREJO-CÓRDOVA, G., LARA, R.H., 2017. *Assessment of biofilm changes and concentration-depth profiles during arsenopyrite oxidation by Acidithiobacillus thiooxidans*. Environ Sci Pollut Res Int., 24, 20082-20092.
- RODRÍGUEZ, A., CASTREJÓN-GODÍNEZ, M.L., SALAZAR-BUSTAMANTE, E., GAMA-MARTÍNEZ, Y., SÁNCHEZ-SALINAS, E., MUSSALI-GALANTE, P., TOVAR-SÁNCHEZ, E., ORTIZ-HERNÁNDEZ, M.L., 2020. *Omics Approaches to Pesticide Biodegradation*. Curr Microbiol, 77(4), 545-563.
- RUAN, Y., HE, D., CHI, R., 2019. *Review on Beneficiation Techniques and Reagents Used for Phosphate Ores*. Minerals, 9, 253.
- SAADELDIN, I.M., SWELUM, A.A.A., ELSAFADI, M., MAHMOOD, A., OSAMA, A., SHIKSHAKY, H., ALFAYEZ, M., ALOWAIMER, A.N., MAGDELDIN, S., 2020. *Thermotolerance and plasticity of camel somatic cells exposed to acute and chronic heat stress*. Journal of advanced research, 22, 105-118.
- SAMREEN, S., KAUSAR, S., 2019. *Phosphorus Fertilizer: The original and commercial sources*. In Phosphorus-Recovery and Recycling, ZHANG, T., IntechOpen, 1-14.
- SARVAMANGALA, H., VINAY, B., GIRISHAL, S.T., 2017. *Bio-beneficiation of Oxide Minerals from Bacillus subtilis Using FTIR and MALDI-TOF Techniques*. J. of Envir. Prot., 8, 194-205.
- SELIM, K.A., ROSTOM, M., 2018. *Bioflocculation of (Iron oxide-Silica) system using Bacillus cereus bacteria isolated from Egyptian iron ore surface*. Egyptian Journal of Petroleum, 27(2), 235-240.
- SMITH, R.W., MIETTINEN, M., 2006. *Microorganisms in flotation and flocculation: future technology or laboratory curiosity?*. Minerals Engineering, 19(6-8), 548-553.
- SUHR, M., LEDERER, F.L., GÜNTHER, T.J., RAFF, J., POLLMANN, K., 2016. *Characterization of Three Different Unusual S-Layer Proteins from Viridibacillus arvi JG-B58 That Exhibits Two Super-Imposed S-Layer Proteins*. PLoS-ONE, 11(6), 1-18.

- TENG, Q., FENG, Y., LI, H., 2018. *Effects of silicate-bacteria pretreatment on desilicization of magnesite by reverse flotation*. Colloids and Surfaces A: Physicochemical and Engineering Aspects, 544, 60-67, ISSN 0927-7757,
- TSHIKANTWA, T.S., ULLAH, M.W., HE, F., YANG, G., 2018. *Current trends and potential applications of microbial interactions for human welfare*. Frontiers in Microbiology, 9(1156), 1-9.
- VIJAYALAKSHMI, S.P., RAICHUR, A.M., 2003. *The utility of Bacillus subtilis as a bioflocculant for fine coal*. Colloids and Surfaces B: Biointerfaces, 29(4), 265-275.
- VOGEL, M., MATYS, S., LEHMANN, F., DROBOT, B., GÜNTHER, T., POLLMANN, K., RAFF, J., 2017. *Use of specific metal binding of self-assembling S-layer proteins for metal bioremediation and recycling*. Solid State Phenomena, 262, 389-393.
- VU, B., CHEN, M., CRAWFORD, R.J., IVANOVA, E.P., 2009. *Bacterial extracellular polysaccharides involved in biofilm formation*. Molecules, 14(7), 2535-2554.
- YANG, Y., RAM, R., MCMASTER, S.A., POWNCEBY, M.I., CHEN, M., 2021. *A comparative bio-oxidative leaching study of synthetic U-bearing minerals: Implications for mobility and retention*. Journal of Hazardous Materials, 403, 123914.
- YAP, H.J., YONG, S.N., CHEAH, W.Q., CHIENG, S., KUAN, S.H., 2020. *Bioleaching of kaolin with Bacillus cereus: Effects of bacteria source and concentration on iron removal*. Journal of Sustainability Science and Management, 15(4): 91-99.
- YU, Z., TIAN, R., LIU, D., ZHANG, Y., LI, H., 2020. *Aggregation kinetics of binary systems containing kaolinite and Pseudomonas putida induced by different 1: 1 electrolytes: specific ion effects*. PeerJ Physical Chemistry, 2, e12.
- ZAIDI, T.S., ZAIDI, T., PIER, G.B., 2018. *Antibodies to Conserved Surface Polysaccharides Protect Mice Against Bacterial Conjunctivitis*. Invest Ophthalmol Vis Sci., 59(6), 2512-2519.